Available online at www.sciencedirect.com

SCIENCE DIRECT®

Diamond & Related Materials 14 (2005) 907–912

DIAMOND AND RELATED MATERIALS

www.elsevier.com/locate/diamond

Nanofabrication and properties of the highly oriented carbon nanocones

W.H. Wang, Y.T. Lin, C.T. Kuo*

Department of Materials Science and Engineering, National Chiao Tung University, Hsinchu, Taiwan

Available online 30 November 2004

Abstract

A process to fabricate Co-assisted carbon nanocones (CNCs) was successfully developed by using microwave plasma chemical vapor deposition (MP-CVD). The nanostructures could be manipulated by adjusting the ratios of the source gases (CH_4/H_2=5/80–15/80 sccm/sccm) and the substrate bias (0~−300 V). The properties of deposited nanostructures were characterized by field emission scanning electron microscopy (FESEM), Raman Spectroscopy, auger electron spectroscopy (AES) spectra. The results show that the nanostructures with cone shape are resulted from competition between the ion bombardment rate and the growing speed of the nanostructures in the plasma, where ion bombardment is drove by the presence of negative substrate bias. In other words, a higher substrate negative bias (>−150 V) and a lower concentration of carbon species in the plasma are favorable conditions to grow highly oriented CNCs due to a greater ion bombardment energy and lower lateral growth rate of the nanostructures, respectively. The results indicate that CNCs synthesized under the applied bias of −300 V show an excellent performance in field emission current density (up to ~173 mA/cm^2 at 10 V/μm).

Keywords: Microwave plasma (MP); Chemical vapor deposition (CVD); Carbon nanocones (CNCs); Field emission (FE)

1. Introduction

Applications of carbon nanostructures, e.g. carbon nanotubes (CNTs), carbon nanocones (CNCs), have been studied for many years due to their higher aspect ratio at the tips, excellent mechanical properties and chemical stability, especially for field emission display (FED) devices. Samsung [1] had successfully fabricated a prototype of 4.5 in. full-color CNT-field emission display with brightness reaching 1800 cd/cm^2 at electrical field of 3.7 V/μm. This amazing result has attracted much attention. Many researches are focused on developing a self-assembly process to fabricate the carbon nanostructures with sharp apex angle to enhance their field emission properties, e.g. carbon nanocones (CNCs) [2–8]. Many reports indicate that the turn on electric field of CNCs can be as low as 0.1–1.38 V/μm due to a larger field enhancement factor β, which are much better than CNTs [9–12]. Furthermore, the cone-shape structure provides higher mechanical and thermal stability than a narrow cylinder structure of CNTs [13]. It was reported that the CNCs can be synthesized under low substrate temperatures (~200 °C) [14], implying its IC compatible fabrication process due to lower temperatures, which are much lower than the temperatures of ~600 °C for CNTs growth. Hence, the CNCs have demonstrated a greater potential and practicability to realize the applications in electronic devices.

In this paper, we report a process to fabricate high-oriented CNCs and study their nanostructures, properties and growth mechanisms. Their field emission properties were emphasized.

2. Experimental

The high-oriented CNCs were synthesized on Si wafer by using catalyst-assisted microwave plasma chemical vapor deposition (MP-CVD) with H_2 and CH_4 as source gases.

* Corresponding author. Tel.: +886 3 5731 949; fax: +886 3 5724 727.
E-mail address: ctkuo@mail.nctu.edu.tw (C.T. Kuo).

0925-9635/$ - see front matter © 2004 Elsevier B.V. All rights reserved.
doi:10.1016/j.diamond.2004.10.013

Table 1
Specimen designation of the as-grown CNCs on silicon wafer and their process conditions

Specimen designation	Ratio of H_2/CH_4 (sccm/sccm)	Substrate temperature (°C)	Deposition time (min)	Bias (V)
B1	80/5	624	10	0
B2		644		−50
B3		637		−150
B4		640		−200
B5		646		−300
B6	80/1	645	10	−200
B7	80/5	640		
B8	80/10	622		
B9	80/15	617		

Substrate: 10 nm cobalt-coated silicon [(100) P-type] wafer. Other CNCs deposition conditions: pressure, 9 Torr; microwave power, 800 W.

Cobalt film with thickness of 10 nm was first deposited on Si wafer by physical vapor deposition (PVD) to act as catalyst. The H-plasma (H_2 flow rate=100 sccm) was utilized for 10 min to activate the Co film to become the well-distributed nano-particles with size distribution between 40 and 95 nm. Then, the wafer with nano-particles on the surface was used to synthesize the carbon nanostructures by MP-CVD at about 600 °C temperature for 10 min and varying H_2/CH_4 ratio and substrate bias. The process parameters and conditions of CNCs are listed in Table 1.

The nanostructures of the deposited CNCs were characterized by field emission scanning electron microscopy (FESEM), transmission electron microscopy (TEM) and high resolution transmission electron microscopy (HRTEM). The bonding structure of the deposited CNCs was studied by Raman spectroscopy (Jobin Yvon LABRAM HR) with 632.8 nm He–Ne laser. Auger electron spectroscopy (AES) (VG Microlab 310F with a Schottky field emission electron source) was used for chemical analysis of CNCs. Field emission properties of as-growth carbon nanostructures were analyzed by *I–V* detector (Keithley 237), and the distance between anode and cathode (CNTs) was set at about 100 μm. The lifetime test of field emitters was examined by current versus time

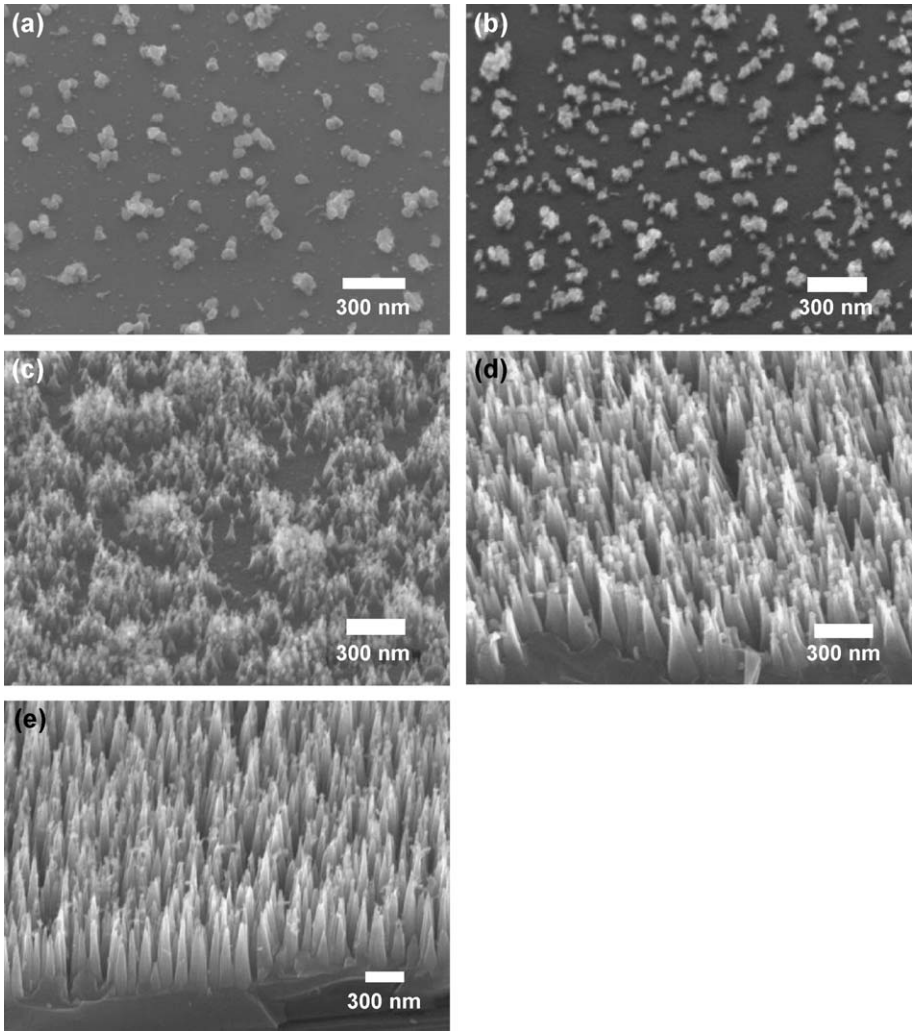

Fig. 1. Typical SEM micrographs of the as-grown CNCs synthesized under different negative substrate bias: (a) 0 V, (b) −50 V, (c) −150 V, (d) −200 V and (e) −300 V (ref. to Table 1).

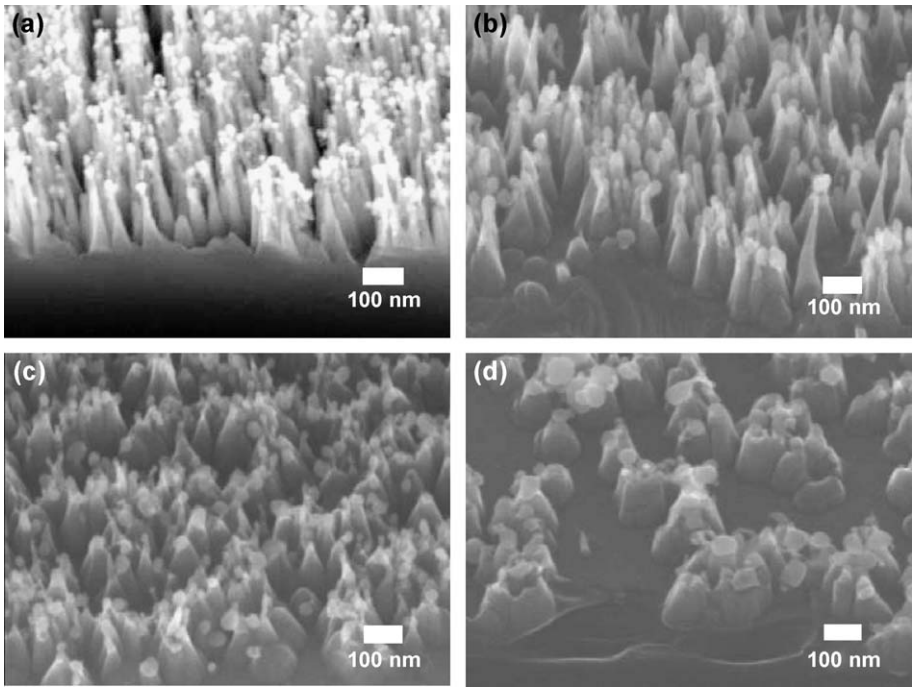

Fig. 2. Typical SEM micrographs of the as-grown CNCs synthesized under different CH_4 flow rates at 80 sccm H_2: (a) 1, (b) 5, (c) 10 and (d) 15 sccm CH_4 (refer to Table 1).

(I–t curve) measurement, where 900 V bias was applied during the 3600 s of operation.

3. Results and discussion

3.1. Effects of applied bias and H_2/CH_4 ratio on the growth of CNCs

The effect of the substrate bias on carbon nanostructures was explored by varying bias from 0 to −300 V under the same H_2/CH_4 ratio (=80/5 sccm/sccm) of the gas sources. The SEM morphologies of the as-grown nanostructures under five different bias values are shown in Fig. 1(a) to (e), respectively. It indicates that the nanostructures gradually change from polyhedral carbon clusters to needle-like CNCs by increasing the negative substrate bias, and become the well-aligned CNCs at bias >−150 V (Specimen B4 and B5). In other words, the substrate bias is one of the key parameters to form the aligned CNCs. Besides, the average height of the CNCs increases from 20–80 to 500 nm as the applied bias increasing from −150 to −300 V. It implies that a greater negative substrate bias can enhance the growth rate of CNCs perpendicular to the substrate. Furthermore, higher substrate bias may promote to form

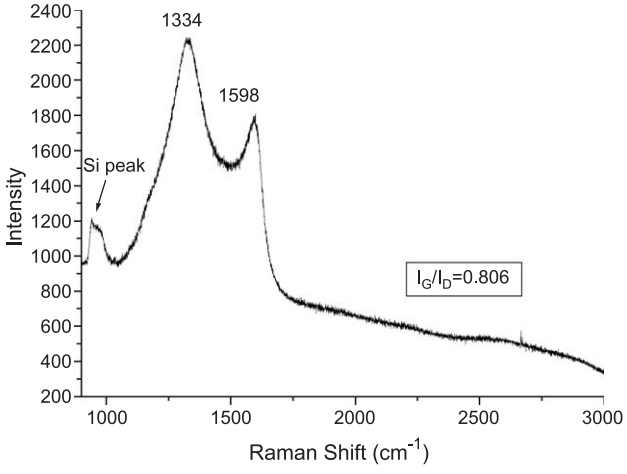

Fig. 3. Raman spectrum of the as-grown CNCs (Specimen B5).

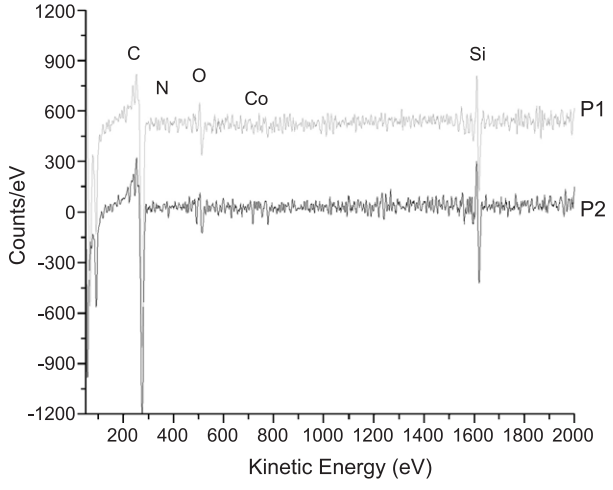

Fig. 4. AES spectra of the as-grown CNCs, where P1 and P2 are sites on individual CNC of the corresponding SEM image in Fig. 5 (Specimen B5).

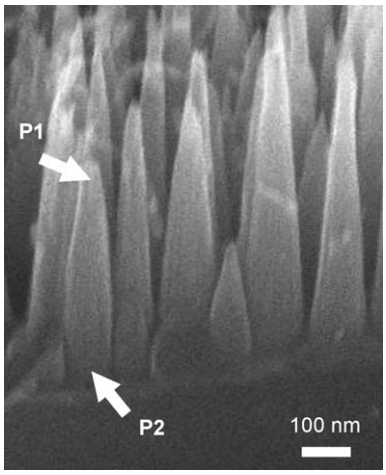

Fig. 5. Typical SEM image of the as-grown CNCs, where the arrowheads indicate the selected tip (P1) and bottom (P2) positions on individual CNC.

the CNCs with sharper tip due to the effect of ions bombardment. This phenomenon is in agreement with the observation of the smaller apex angle at the tips of CNCs, where the apex angles are 15–20° and 9–12° under −200 V (specimen B4) and −300 V (specimen B5) applied bias, respectively.

The SEM morphologies of the as-grown CNCs synthesized under different H_2/CH_4 ratios of 80/1, 80/5, 80/10, and 80/15 sccm/sccm are shown in Fig. 2(a) to (d), respectively. It indicates the CNCs with a greater average apex angle and larger bottom diameters are deposited under a lower H_2/CH_4 ratio in gas sources. In other words, the higher concentration of CH_4 gas may lead to an increase of the lateral growth rate of CNCs to form a blunt apex angle. The results imply that the nanostructures of CNCs are determined essentially by the competition among etching rate of plasma species, the lateral growth rate and the upward deposition rate of carbon along the surface or through the interior of the catalysts. It is interesting to note that CH_4 concentration adopted to the as-grown CNCs in these cases are between the concentrations

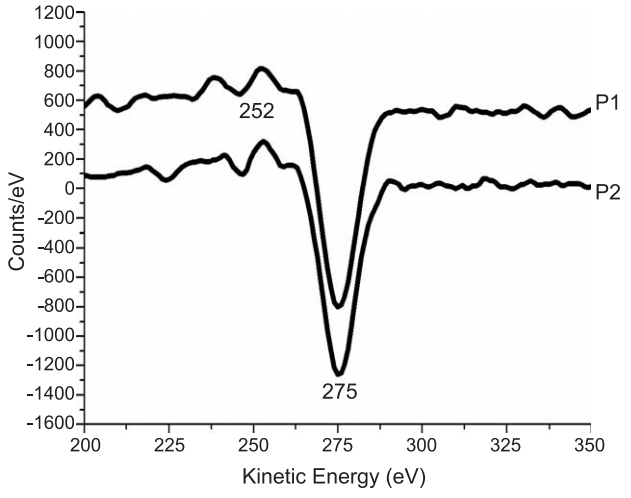

Fig. 6. The magnified AES spectra of Fig. 4 around carbon peak positions.

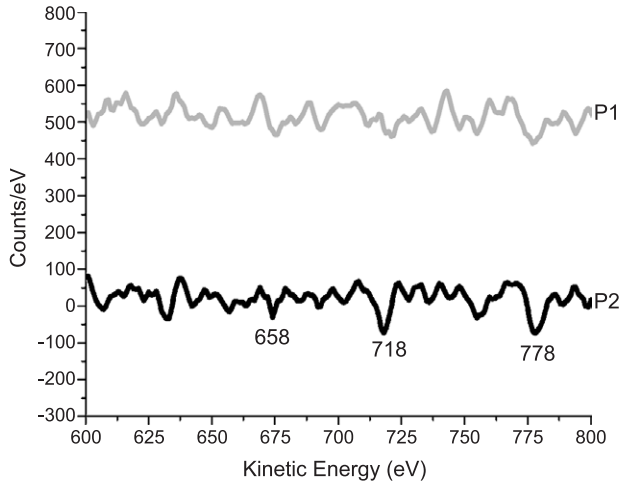

Fig. 7. The magnified AES spectra of Fig. 4 around Co peak positions.

for growth of diamond film and CNTs, where diamond film deposition require a lower concentration (H_2/CH_4=~100/5 sccm/sccm) [15,16]. It is concluded that highly oriented CNCs are more likely to be formed under the appropriate concentration of carbon species in the plasma and higher negative substrate bias.

3.2. Raman and AES analyses of the as-grown CNCs

The Raman spectrum of the as-grown CNCs is shown in Fig. 3 (Specimen B5). The peak position of the D band and G band are around 1334 and 1598 cm^{-1}, respectively, where the I_G/I_D ratio is ~ 0.81. Huang's group proposed that a shift of the $E_{2g}G$ mode from its normal value of 1580 to 1598 cm^{-1} is an indication of the existence of nanocrystalline graphite or sp^2 clusters [17–19]. The peak at 1334 cm^{-1} is assigned as A_{1g} mode due to the presence of aromatic rings in disordered graphite rather than diamond peak at 1332 cm^{-1}. Therefore, the bonding structure of the as-grown CNCs can be considered as sp^2 clusters in an amorphous carbon (a:C) matrix.

The AES spectra and the corresponding SEM image of the as-grown CNCs at the tip (P1) and bottom (P2) sites are shown in Figs. 4 and 5, respectively (Specimen B5). The results show detectable signals of carbon, nitrogen, oxygen, cobalt and silicon both on the tip and bottom surfaces of the CNCs. It speculates that the signals of oxygen and nitrogen

Table 2
FE properties of the as-grown nanostructures synthesized under different negative substrate bias

Specimen designation	Applied bias (V)	$E_{turn\text{-}on}$ at 10 μA/cm^2 (V/μm)	$E_{threshold}$ at 10 mA/cm^2 (V/μm)	Current density at 10 V/μm (mA/cm^2)
B2	−50	7.6	not reach	0
B3	−150	8.3	not reach	0
B4	−200	5.8	8.1	59
B5	−300	5.0	7.0	173

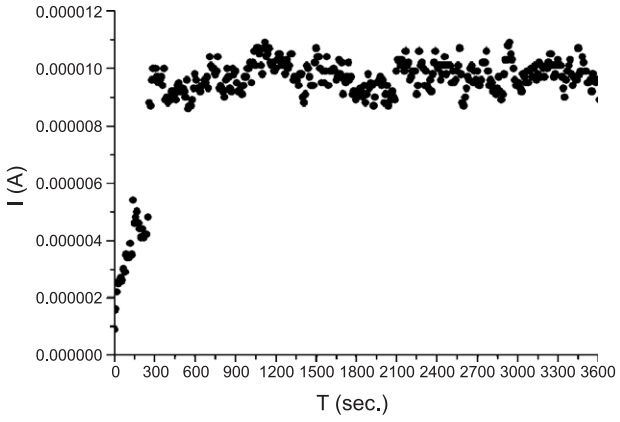

Fig. 8. The *I–t* lifetime testing curve of the as-grown CNCs under 900 V (Specimen B5).

may be attributed to absorption from atmosphere during specimen handling. The corresponding AES magnified spectra of Fig. 4 are shown in Figs. 6 and 7 to compare with the reported spectrum [20,21]. It indicates that the peaks of the as-grown CNCs at 252 and 275 eV are belonging to graphite phase. It is also noted that the peaks for Co catalyst at tip area are slightly weaker than at bottom area, implying special growth mechanism combining both base-growth and tip-growth modes.

Moreover, it is interesting to note that the significant Si signal is present in the AES spectra of the as-grown CNCs. First, it may be due to the bias induced Si sputtering from the Si substrate and re-depositing on the surface [22]. Secondly, the diffusion of Si atoms along the CNCs surface from Si substrate may occur [23]. In other words, the nanostructure of the as-grown CNCs is basically consisting of mixture of Co, graphene planes, disordered graphite, amorphous Si and amorphous carbon.

3.3. Field emission properties

The field emission properties of the as-grown CNCs deposited with different negative substrate biases (Specimens B2, B3, B4 and B5) are shown in Table 2. It shows that the best FE properties belong to the CNCs by the greatest negative bias (−300 V, Specimen B5), which is essentially the CNCs of the greatest aspect ratio; where the turn on electric field ($E_{\text{turn-on}}$), threshold electric field (E_{th}) and the current density (at 10 V/μm) are 5.0 V/μm, 7.0 V/μm and 173 mA/cm^2, respectively. It is interesting to note that the CNCs at a relative lower negative bias than −300 V show the agglomeration phenomenon of CNCs (Specimen B4 at −200 V bias), which may further decline the FE properties due to screening effect among neighbor CNCs. The current versus time (*I–t*) curve of the as-grown CNCs at 900 V is used to examine the stability of CNCs during operation, as shown in Fig. 8 (Specimen B5). Except the first 5 min, it indicates that the current remains constant for a testing period of 1 h, though it can be stand longer, implying good adhesion between CNCs with the substrate. The rising of emission current during the first 5 min is due to removal of the loose nanostructures and annealing effect by the intense electric field.

4. Conclusions

By manipulating the H_2/CH_4 ratio and applying sufficient applied negative bias (≧−200 V), the well-aligned CNCs were successfully synthesized by Co-assisted MP-CVD method. The results show that CNCs are basically consisting of mixture of Co particles, graphene planes, disordered graphite, amorphous Si and amorphous carbon. It is found that a greater negative substrate bias can give rise to better-aligned CNCs with sharper apex angle at the tips, better FE properties, greater adhesion with the substrate and better structure stability in electric field. It is also found that the CNCs under −200 V bias has agglomeration phenomenon, which will have a negative effect to FE properties due to screening effect. Under the present conditions, the well-aligned CNCs synthesized under H_2/CH_4 (80/5 sccm/sccm) ratio, −300 V applied bias and 10 min deposition time exhibit good life testing stability and best FE properties: $E_{\text{turn-on}}$ ~5.0 V/μm, E_{th} ~7.0 V/μm, and J ~173 mA/cm^2 at 10 V/μm.

Acknowledgements

This work was supported by the National Science Council of Taiwan under Contract No. NSC92-2216-E-009-010, NSC92-2216-E-009-009, and NSC92-2210-M-009-001.

References

[1] W.B. Choi, D.S. Chung, J.H. Kang, H.Y. Kim, Y.W. Jin, I.T. Ha, Y.H. Lee, J.E. Jung, N.S. Lee, G.S. Park, J.M. Kim, Appl. Phys. Lett. 75 (1999) 3129.
[2] J. Jang, S.J. Chung, H.S. Kim, Appl. Phys. Lett. 79 (2001) 1682.
[3] C.L. Tsai, C.F. Chen, C.L. Lin, Appl. Phys. Lett. 80 (2002) 1821.
[4] C.J. Huang, Y.K. Chih, J. Hwang, J. Appl. Phys. 94 (2003) 6796.
[5] Y.T. Jan, H.C. Hsieh, C.F. Chen, Diamond Relat. Mater. 8 (1999) 772.
[6] C.R. Lin, T.J. Wang, K.C. Chen, C.H. Chang, Mater. Chem. Phys. 72 (2001) 126.
[7] G. Zhang, X. Jiang, E. Wang, Science 300 (2003) 472.
[8] Y. Hayashi, T. Tokunaga, T. Soga, T. Jimbo, Appl. Phys. Lett. 84 (2004) 2886.
[9] J.S. Jang, J. Chung, H.S. Kim, Appl. Phys. Lett. 79 (2001) 1682.
[10] H.C. Lo, D. Das, J.S. Hwang, K.H. Chen, C.H. Hsu, C.F. Chen, L.C. Chen, Appl. Phys. Lett. 83 (2003) 1420.
[11] C.L. Tsai, J.H. Hsu, C.F. Chen, Appl. Phys. Lett. 82 (2003) 4337.
[12] C.J. Huang, Y.K. Chih, J. Hwang, J. Appl. Phys. 94 (2003) 6796.
[13] V.I. Merkulov, A.V. Melechko, M.A. Guillorn, D.H. Lowndes, M.L. Simpon, Chem. Phys. Lett. 350 (2001) 381.
[14] X.W. Liu, C.H. Lin, L.T. Chao, H.C. Shih, Mater. Lett. 44 (2000) 304.
[15] H.L. Chang, C.H. Lin, C.T. Kuo, Diamond Relat. Mater. 11 (2002) 793.
[16] C.M. Hsu, Master Thesis, (2002), Mat. Res. Lab. MSE, NCTU.
[17] C.J. Huang, Y.K. Chih, J. Hwang, J. Appl. Phys. 94 (2003) 6796.
[18] A.C. Ferrari, J. Robertson, Phys. Rev., B 61 (2000) 14095.

[19] R.O. Dillon, J.A. Woollam, V. Katkanant, Phys. Rev., B 29 (1984) 3482.
[20] C.R. Lin, T.J. Wang, K.C. Chen, C.H. Chang, Mater. Chem. Phys. 72 (2001) 126.
[21] I.F. Ferguson, Auger Microscope Analysis, IOP, Publishing, Bristol, 1998, p. 63.
[22] X.D. Bai, C.Y. Zhi, S. Liu, E.G. Wang, Z.L. Wang, Solid State Commun. 125 (2003) 185.
[23] W.Y. Yeh, J.Y. Hwang, A.P. Lee, C.S. Kuo, H. Chang, Appl. Phys. Lett. 79 (2001) 3609.